Lobe cell convection and field-aligned currents poleward of the region 1 current system

S. Eriksson,[1] J. W. Bonnell,[2] L. G. Blomberg,[1] R. E. Ergun,[3] G. T. Marklund,[1] and C. W. Carlson[2]

Received 5 June 2001; revised 17 September 2001; accepted 16 October 2001; published 15 August 2002.

[1] We present a case and statistical study of plasma convection in the Northern Hemisphere during summer conditions using electric field, magnetic field, and particle data taken during dawn-dusk directed orbits of the FAST satellite. To our knowledge, this set provides the most comprehensive combination of data as yet presented in support of lobe cell convection from an ionospheric perspective this far from the noon sector. In particular, we study the current systems and convection patterns for all passes in July 1997 that show evidence for six large-scale field-aligned currents (FACs) rather than the usual system of four FACs associated with the region 1/region 2 current systems. A total of 71 passes out of 232 in the study had the extra pair of FACs. The extra pair of FACs in 30 of the 71 cases lies either on the dawnside or on the duskside of the noon-midnight meridian, and their position is strongly correlated with the polarity of the IMF B_y (negative and positive, respectively). This is consistent with the IMF dependence of a three-cell convection pattern of coexisting merging, viscous, and lobe-type convection cells. The occurrence of the asymmetric FAC pair was also strongly linked to conditions of IMF $|B_y/B_z| > 1$. The extra pair of FACs in these cases was clearly associated with the lobe cell of the three-cell convection system. The remaining 41 cases had the pair of FACs straddling the noon-midnight meridian. The extra pair of FACs was often (20 cases out of 30) observed at magnetic local times more than three hours away from noon, rather than being confined to regions near noon and the typical location of the cusp. Such a current system consisting of a pair of FACs poleward of the nearest region 1 current is consistent with the IMF B_y-dependent global MHD model developed by *Ogino et al.* [1986] for southward IMF conditions, as well as with other magnetospheric and ionospheric convection models that include the effects of merging occuring simultaneously at both low-latitude dayside and high-latitude lobe and flank magnetopause reconnection sites. Finally, the presence of the additional FACs and three-cell convection well away from noon show that the entire dayside ionosphere is affected by IMF-dependent processes, rather than only a limited region around noon. *INDEX TERMS:* 2760 Magnetospheric Physics: Plasma convection; 2708 Magnetospheric Physics: Current systems (2409); 2784 Magnetospheric Physics: Solar wind/magnetosphere interactions; 2431 Ionosphere: Ionosphere/magnetosphere interactions (2736); *KEYWORDS:* lobe reconnection

1. Introduction

[2] The field-aligned current system at high latitudes has been studied for several decades, with the first systematic description being that of *Iijima and Potemra* [1976], who identified the large-scale statistical pattern of field-aligned currents known as the region 1 and region 2 current systems. The region 1/2 current systems are simplest in form across the dawn-dusk meridian, especially under conditions of southward interplanetary magnetic field (IMF $B_z < 0$). The equatorward portion of the FAC system (region 2) is downward on the duskside and upward on the dawnside, while the poleward portion of the FAC system (region 1) is upward on the duskside and downward on the dawnside.

[3] This large-scale, two-region pattern of FACs is not the only current system seen at higher latitudes, however. Past studies have reported on large-scale field-aligned currents (FACs) poleward of the region 1 current system. These FACs have been referred to as the cusp FAC system [*Iijima and Potemra*, 1976; *Iijima et al.*, 1978], mantle currents [*Bythrow et al.*, 1988], or as the "midday region 0" current system near noon [*Heikkila*, 1984; *Ohtani et al.*, 1995a].

[1]Alfvén Laboratory, Royal Institute of Technology, Stockholm, Sweden.
[2]Space Sciences Laboratory, University of California, Berkeley, California, USA.
[3]Laboratory for Atmospheric and Space Physics, University of Colorado, Boulder, Colorado, USA.

0148-0227/02/2001JA005041$09.00

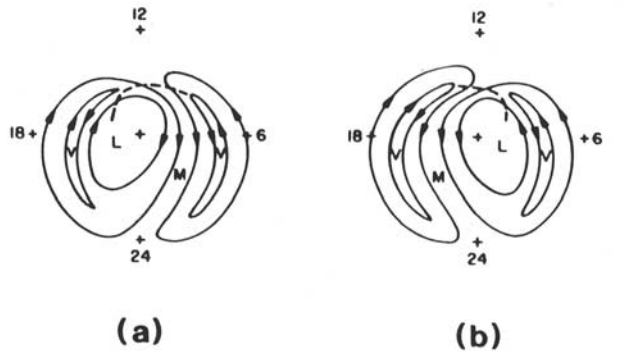

Figure 1. Global ionospheric convection model for southward IMF from *Burch et al.* [1985]. This Figure is adapted from *Burch et al.* [1985]. Three types of convection cells are suggested, denoted "M" for a merging cell, "L" for a lobe cell, and "V" for a viscous cell. Three convection reversals can be seen (a) on the duskside for positive IMF B_y and (b) on the dawnside for negative IMF B_y.

[4] *Cattell et al.* [1979] studied S3-3 auroral zone crossings and found an additional upward current sheet poleward of the oppositely directed region 1 current in approximately 30% of the dawnside cases. It was stressed that this third current sheet, though present in some published magnetic field plots, was not mentioned in papers based on Triad satellite data. The same observation was made by *Bythrow et al.* [1987], stating that satellites such as Triad, ISIS 2, and Magsat all showed evidence of this upward FAC in the magnetic field data without it being reported [*Iijima and Potemra*, 1976; *McDiarmid et al.*, 1978; *Zanetti and Potemra*, 1982]. *Bythrow et al.* [1987] reported a dual-satellite observation of this dawnside upward FAC made by Viking at 0850 MLT and DMSP-F7 at 0630 MLT, supporting the suggestion of a flankward continuation of the cusp currents proposed by *Heikkila* [1984].

[5] Using magnetic field and plasma data from 47 passes of the Dynamics Explorer 2 (DE 2) satellite, *Taguchi et al.* [1993] examined the interplanetary magnetic field (IMF) B_y dependence of FACs in the near-noon region. The orbits were selected from a total period of approximately eight months of DE 2 data collection, on the conditions that cleft particles were detected and that the IMF satisfied the criteria $|B_y| \geq 5$ nT and $|B_z| \leq 5$ nT. They found 20 examples with positive IMF B_y having a pair of large-scale FACs poleward of the region 1 current system. The equatorward current was flowing into the ionosphere while the poleward FAC was directed out of the ionosphere. The opposite current flows were observed for another 27 cases with negative IMF B_y (see their Figure 7). The current directions were found to be independent of the IMF B_z polarity. A qualitative model was presented to explain the IMF B_y-dependent near-noon pair of FACs as being generated on open field lines recently reconnected on the dayside magnetopause. No electric field data were included in the study, and so the relationship of this pair of large-scale FACs to the ionospheric convection pattern was not explored.

[6] The study of *Ohtani et al.* [1995b] did explore the connection between the dayside FAC systems and ionospheric convection. Using data from both Viking and DMSP-F7 taken within three hours of local noon, they reported four events of a system of four large-scale FAC sheets in the prenoon sector. The four FACs were directed upward, downward, upward, and downward respectively as DMSP-F7 moved poleward. The 1-hour averaged IMF B_y was negative for all four events and the current directions were in agreement with *Taguchi et al.* [1993]. *Ohtani et al.* [1995b] interpreted the IMF B_y dependence based on the global convection model proposed by *Burch et al.* [1985], which consists of coexisting dayside merging, lobe, and viscous type of cells. This explanation was supported in one case by a Viking UV image, and in another case by one component of the Viking electric field [*Marklund et al.*, 1990]. In this three-cell convection model, the high-latitude ionospheric convection is driven by several different processes. The "merging" cell is driven by reconnection at a low-latitude site on the dayside as in the usual, two-cell reconnection-driven model. The "viscous" cell is driven by a viscous process occurring within the low-latitude boundary layer (LLBL). The "lobe" cell is driven by reconnection at a site on the lobe or flank magnetopause. The additional FACs found poleward of the region 1 current systems have been associated with the lobe cell, but it has not been clear how the FACs and associated convection would fit in with the proposed generator region.

[7] Evidence for reconnection of the tail lobe field lines with the IMF was provided by ISEE 2 data at times when large local magnetic field shears were associated primarily with large IMF B_x and B_y components, rather than with the IMF B_z [*Gosling et al.*, 1991; *Gosling et al.*, 1996]. *Phan et al.* [2001] further report a flank magnetopause reconnection event detected by the Wind spacecraft as it moved into the low-latitude dawn tail near $x_{GSE} \sim -10R_E$ southward of the equatorial plane for predominantly positive IMF B_y.

[8] The existence of lobe cells has been demonstrated in the frame of MHD models as well. *Ogino et al.* [1986] applied a three-dimensional MHD simulation code to examine the magnetospheric configuration for negative IMF B_y. A resistive term $\eta\nabla^2\vec{B}$ was introduced which allowed magnetic reconnection to occur in the simulation. They found signatures of localized reconnection on the high-latitude dawnside magnetopause at $x = -18.5\ R_E$ as well as a northward (southward) twist of the dawnside (duskside) plasma sheet. The reconnection site moved equatorward along the dawnside flank magnetopause for increasingly southward IMF. The results were proposed to be symmetric for positive IMF B_y. *Crooker et al.* [1998] have also demonstrated the existence of lobe cells in the frame of an MHD model using a strictly positive IMF B_y.

[9] The presence of a lobe cell adjacent to a viscous type of cell produces three large-scale convection reversals in the duskside (dawnside) polar cap for positive (negative) IMF B_y (see Figure 1) if we assume a gradual transition from antisunward to sunward flow in the outer part of the LLBL [*Siscoe et al.*, 1991]. The most equatorward convection reversal is located inside the "viscous" cell which maps to the assumed stagnation region in the outer LLBL. A second convection reversal exists between the higher-latitude sunward flow of the lobe cell and the lower-latitude antisunward flow of the viscous cell. The third convection reversal is found within the lobe cell.

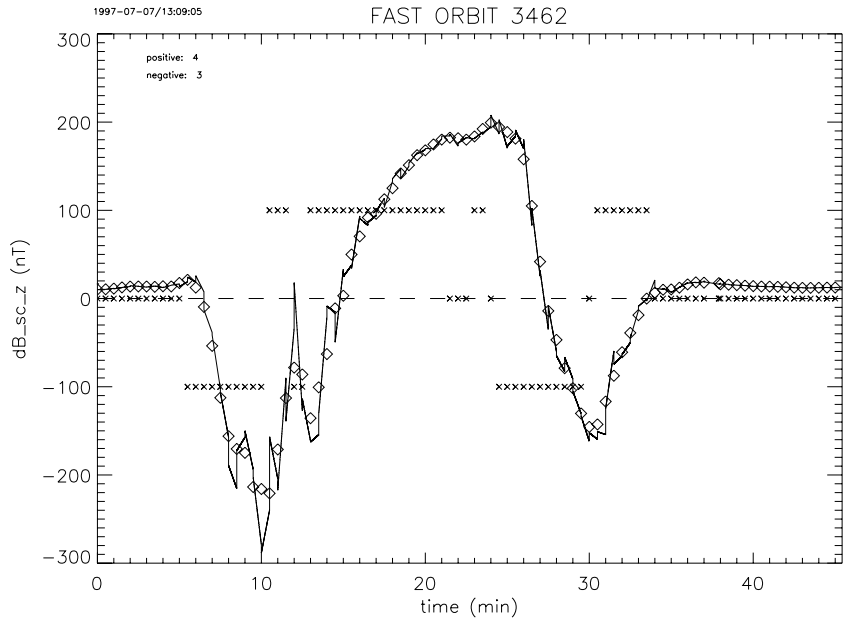

Figure 2. Resulting averaged dB_z perturbation magnetic field from the pattern recognition algorithm for FAST orbit 3462. The algorithm indicated four positive slopes and three negative slopes. Four FACs are observed on the dawnside and two on the duskside after manual inspection.

[10] We present simultaneous electric field, magnetic field, and particle data from dawn-to-dusk low-altitude FAST passes in the Northern Hemisphere for summer conditions, demonstrating a system of four FACs at the dawn or the dusk polar cap auroral edges depending on IMF direction. Occasionally, these FACs are located more than three hours away from local noon, which seems to extend the results found by *Taguchi et al.* [1993] of FACs near noon and to verify the basic features of the MHD model developed by *Ogino et al.* [1986]. The data also generally agree with the global model of ionospheric convection proposed by *Burch et al.* [1985] and *Reiff and Burch* [1985].

2. Instrumentation, Methodology, and Observations

[11] The FAST mission and its scientific payload are described by *Carlson et al.* [1998]. A brief description of the instruments included in this study will be given here. The electron and ion energy spectra are gathered by top-hat electrostatic analyzers. In survey mode (used here), one complete energy-pitch angle spectrum is constructed from the average of 32 individual 70-ms spectra. Spin plane electric field data are gathered at 32 samples/s resolution in slow survey mode, with vector fluxgate magnetometer data gathered at 8 samples/s. Spin fit electric field data are produced every half spin using ground software. The electric potential along the satellite track is obtained by integrating the electric field. A constant electric field is added to the original measurement to force a match between the low-latitude potential at both ends of each polar cap pass. We thereby correct for systematic electric field offsets due in part to inexact satellite attitude determination [see also *Eriksson et al.*, 2000]. The spin plane electric and spin axis magnetic field measurements are used to determine the convection patterns and FAC systems crossed by FAST in this survey.

[12] The height-integrated Pedersen conductivity may be considered uniform in the dayside summer ionosphere, because of the dominant UV contribution to the ionization. Moreover, a high correlation between perpendicular components of the electric and magnetic fields during current sheet crossings implies that field-aligned currents close via Pedersen currents [*Sugiura et al.*, 1982] in the ionosphere. Each convection reversal of a three-cell convection pattern should then coincide with a gradient in the magnetic field that denotes a quasi-steady FAC.

[13] The FAST satellite is spinning in a cartwheel configuration where the spacecraft y axis points along the velocity vector and the z axis points along the spin axis direction, respectively. This means that the y axis points duskward and that the z axis points sunward for the dawn-to-dusk passes studied here. We developed an automated detection algorithm to search for large-scale gradients in the FAST perturbation magnetic field data, using the dB_z component in a spacecraft coordinate system. The contribution of the International Geomagnetic Reference Field (IGRF) to the total magnetic field is subtracted prior to analysis. The detection algorithm includes the following steps. We fit line segments to each 30-s interval of data above 50° invariant latitude (ILat), which corresponds to ~200 km along the orbit. This gave us a smoothed estimate of the perturbation magnetic field. The resulting profile was further smoothed using a 90-s running average filter to remove the discontinuous jumps introduced between each line segment. The commencement of a possible large-scale FAC is indicated by the algorithm if the absolute difference in magnitude between two consecutive intervals is larger than 5 nT. An example is illustrated in Figure 2 where all positive gradients (downward current) are indicated by crosses at the 100 nT level. A negative gradient (upward current) is indicated by crosses at the −100 nT level. Applying the algorithm on 232 dawn-to-dusk FAST passes

in July 1997 followed by manual inspection of those events where the algorithm indicated between six and eight FACs, resulted in 71 events of six large-scale FACs of alternating upward and downward direction along the orbit.

[14] Figures 3, 4, and 5 illustrate three examples where four such FACs were found either completely on the dawnside (Figure 3) or the duskside (Figures 4 and 5). Figures 2 and 6 show the resulting polynomial fit of dB_z for Figures 3 and 4 using the automated algorithm and the possible locations of large-scale FACs. Figures 3 through 5 show five panels of data along the orbit. The top two panels show the spin resolution electric field along the velocity direction with the contribution of the corotation electric field subtracted and the integrated electric field assuming a return to zero potential at subauroral latitudes [*Eriksson et al.*, 2000]. A positive (negative) electric field indicates antisunward (sunward) $\vec{E} \times \vec{B}$ convection. The middle panel shows the cross-track dB_z perturbation magnetic field before the polynomial fit and the along-track dB_y magnetic field perturbation. The last two panels show the energy-time spectrograms of precipitating ions and electrons, respectively, in the pitch angle range of 0–30°. Green vertical lines mark the two most poleward convection reversal boundaries (CRB) associated with either a maximum or a minimum polar cap potential. Red lines mark the two CRBs detected equatorward of either one of those extrema.

[15] The IMF in GSM coordinates corresponding to each polar crossing is retrieved by taking into account the approximate time delay for the solar wind to propagate from the Wind spacecraft to an average magnetopause location of 11 R_E. Wind was located closer than x_{GSE} = 90 R_E in July 1997. A further time delay of 15 min is added to allow for the ionosphere to respond globally to a change in IMF at the magnetopause [*Sanchez et al.*, 1991]. The IMF is then averaged over the preceding 30-min period.

2.1. Case Study

[16] Below we present three events drawn from our statistical study as examples of a system of four large-scale FACs lying either completely on the dawnside or on the duskside of the noon-midnight meridian.

2.1.1. Event 1: 7 July 1997, 1314:00–1345:00 UT (FAST orbit 3462, $B_y < 0$)

[17] For this event the IMF (B_x, B_y, B_z) is directed (1.5, −9.2, −1.5) nT. There is good qualitative agreement between the large-scale electric field and the dB_z perturbation magnetic field which implies four stationary FACs on the dawnside and two current sheets on the duskside (see Figures 2 and 3). The along-track dB_y and the cross-track dB_z components suggest that the low-latitude pair of FAC sheets and the high-latitude pair of FACs are lying at an angle to each other that separates the lower from the higher latitude pairs of FAC and that FAST passes through or near the region where these two planes connect. The integrated electric field suggests a potential drop of about 85 kV between the two large-scale CRBs.

[18] A gradual decrease is observed in dB_z between 1315:18 and 1319:15 UT and corresponds to an upward field-aligned current coincident with sunward convection. The current sheet correlates well with precipitating electrons and ions which are characteristic of plasma sheet origin and its polarity is the same as the dawnside region 2 current.

[19] The decrease in dB_z is followed by an increase (downward current) of almost equal magnitude of about 300 nT over an approximate distance of 800 km at FAST altitude from 1319:15 until 1321:10 UT. A positive gradient in the electric field is observed in the same region, leading to a field reversal from negative to positive just prior to 1321:10 UT. The electric field stays positive for about 15 s or ∼100 km along the orbit, and indicates a narrow region of antisunward convection. The downward current is further associated with structured lower-energy electron precipitation and a gradual decrease of the upper energy cutoff of soft high-energy electrons. The average energy of precipitating ions in the equatorward part of this current from ∼1319:22 to 1320:00 UT is markedly lower than that in the poleward part of the upward directed region 2 current. Particle precipitation in this downward current may be identified with the boundary plasma sheet (BPS) or the LLBL following *Newell et al.* [1991b].

[20] The dawn-dusk component of the electric field switches direction to negative (sunward convection) poleward of the ∼100 km wide region of antisunward convection and stays negative until the third and final CRB on the dawnside to antisunward convection over the polar cap.

[21] The negative gradient in the electric field (from 1321:10 to 1322:30 UT) corresponds to a ∼560 km wide region of $\nabla \cdot \vec{E} < 0$ at FAST altitude. This region further coincides with a noticeable decrease of ∼190 nT in the east-west dB_z component of the perturbation magnetic field which is associated with an upward FAC. The equatorward part of this current is collocated with the convection reversal (red vertical line in Figure 3) to sunward convection. The upward FAC is primarily associated with structured high-energy electron precipitation with increased energy fluxes in the energy range 600 eV to 2.5 keV. Note the presence of a narrow ∼30 s (∼210 km) wide region of ∼6 keV ion precipitation that seems to coincide with locally increased $\nabla \cdot \vec{E} < 0$ and enhanced sunward convection. The energy flux of these ions is lower by an order of magnitude as compared with the ion precipitation just poleward of the upward region 2 current. We identify the region of upward current and $\nabla \cdot \vec{E} < 0$ with particle precipitation characteristic of the LLBL [*Newell et al.*, 1991b] mainly on sunward convecting plasma.

[22] The integrated electric field indicates a local maximum in the ionospheric potential of ∼44 kV at ∼1323:00 UT (green vertical line in Figure 3) which marks the

Figure 3. (opposite) FAST orbit 3462. The panels display (from top to bottom): the along-track electric field and electric potential (assuming return to zero potential at low latitudes), the cross-track dB_z (green) and along-track dB_y (red) perturbation magnetic fields in a spacecraft coordinate system, and the precipitating ions and electrons, respectively. A green vertical line marks the maximum and minimum electric potential. A red line marks any CRB equatorward of these. Four FACs are observed on the dawnside for IMF B_y = −9.2 nT. See color version of this figure at back of this issue.

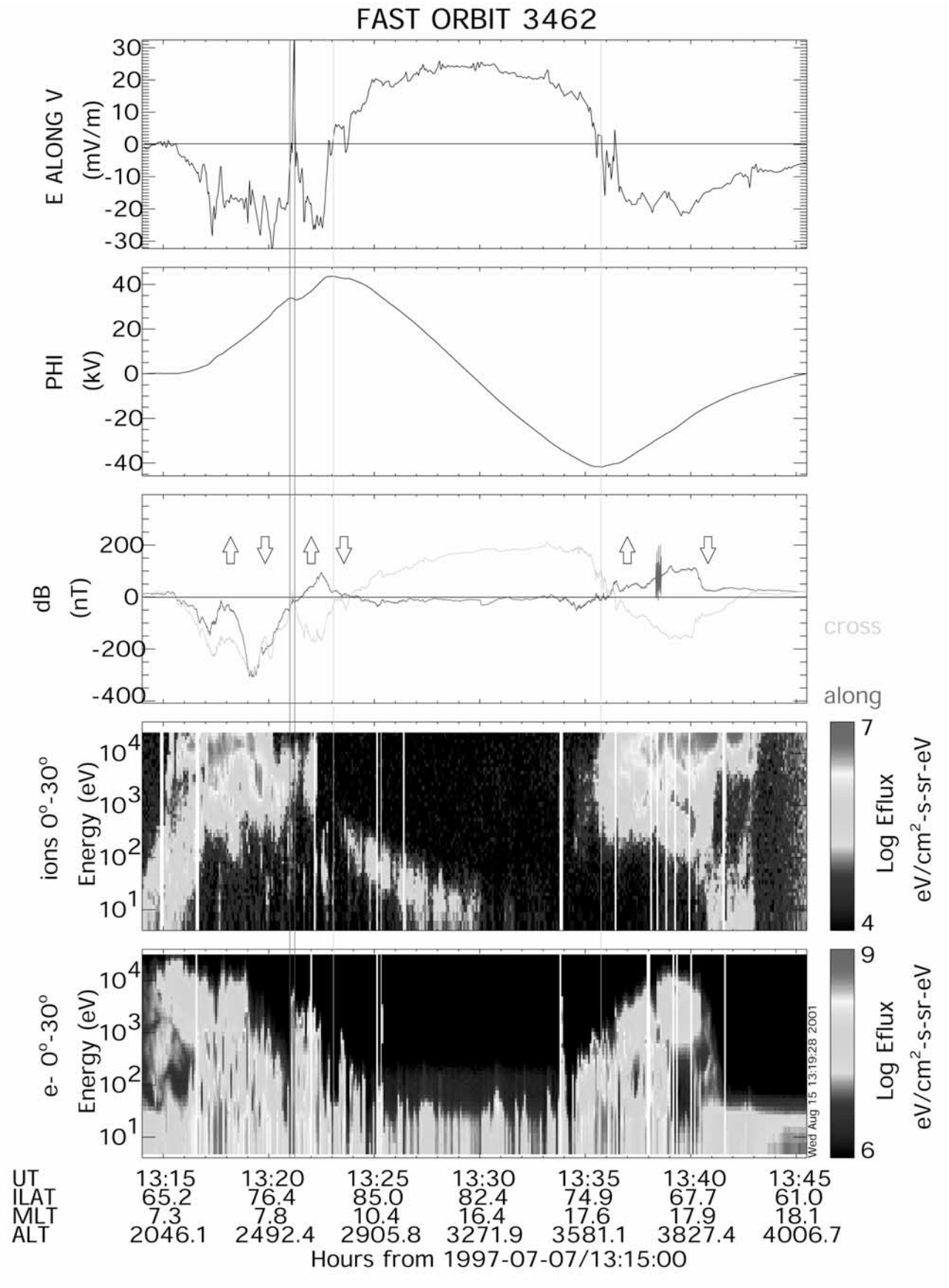
FAST ORBIT 3462
E ALONG V
(mV/m)
30
20
10
0
-10
-20
-30
PHI
(kV)
40
20
0
-20
-40
dB
(nT)
200
0
-200
-400
cross
along
ions 0°-30°
Energy (eV)
10^4
10^3
10^2
10^1
Log Eflux
eV/cm^2-s-sr-eV
7
4
e- 0°-30°
Energy (eV)
10^4
10^3
10^2
10^1
Log Eflux
eV/cm^2-s-sr-eV
9
6
Wed Aug 15 13:19:28 2001
UT 13:15 13:20 13:25 13:30 13:35 13:40 13:45
ILAT 65.2 76.4 85.0 82.4 74.9 67.7 61.0
MLT 7.3 7.8 10.4 16.4 17.6 17.9 18.1
ALT 2046.1 2492.4 2905.8 3271.9 3581.1 3827.4 4006.7
Hours from 1997-07-07/13:15:00

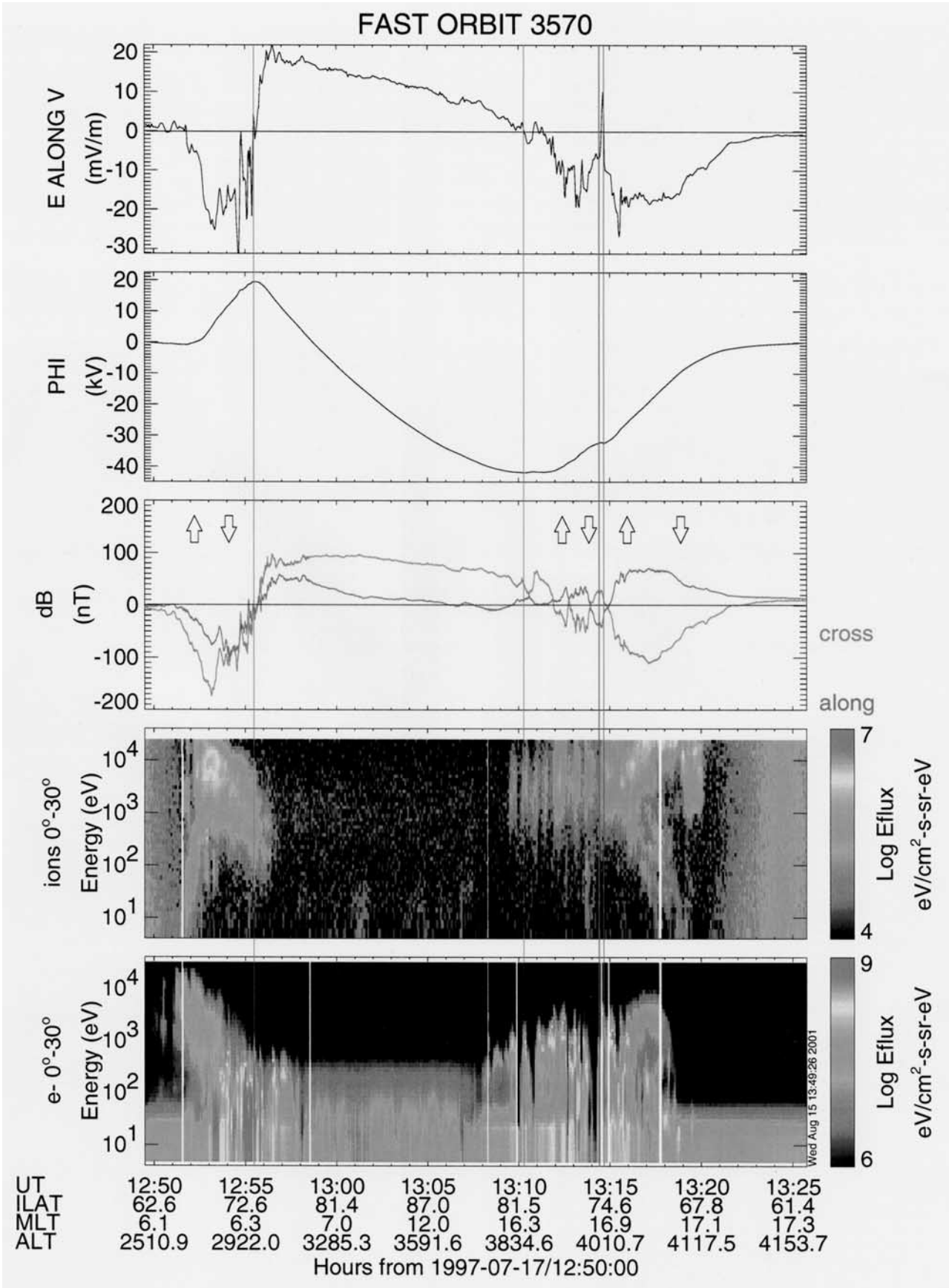

Figure 4. FAST orbit 3570. Same format as Figure 3. Four FACs are observed on the duskside for IMF B_y = 3.9 nT. See color version of this figure at back of this issue.

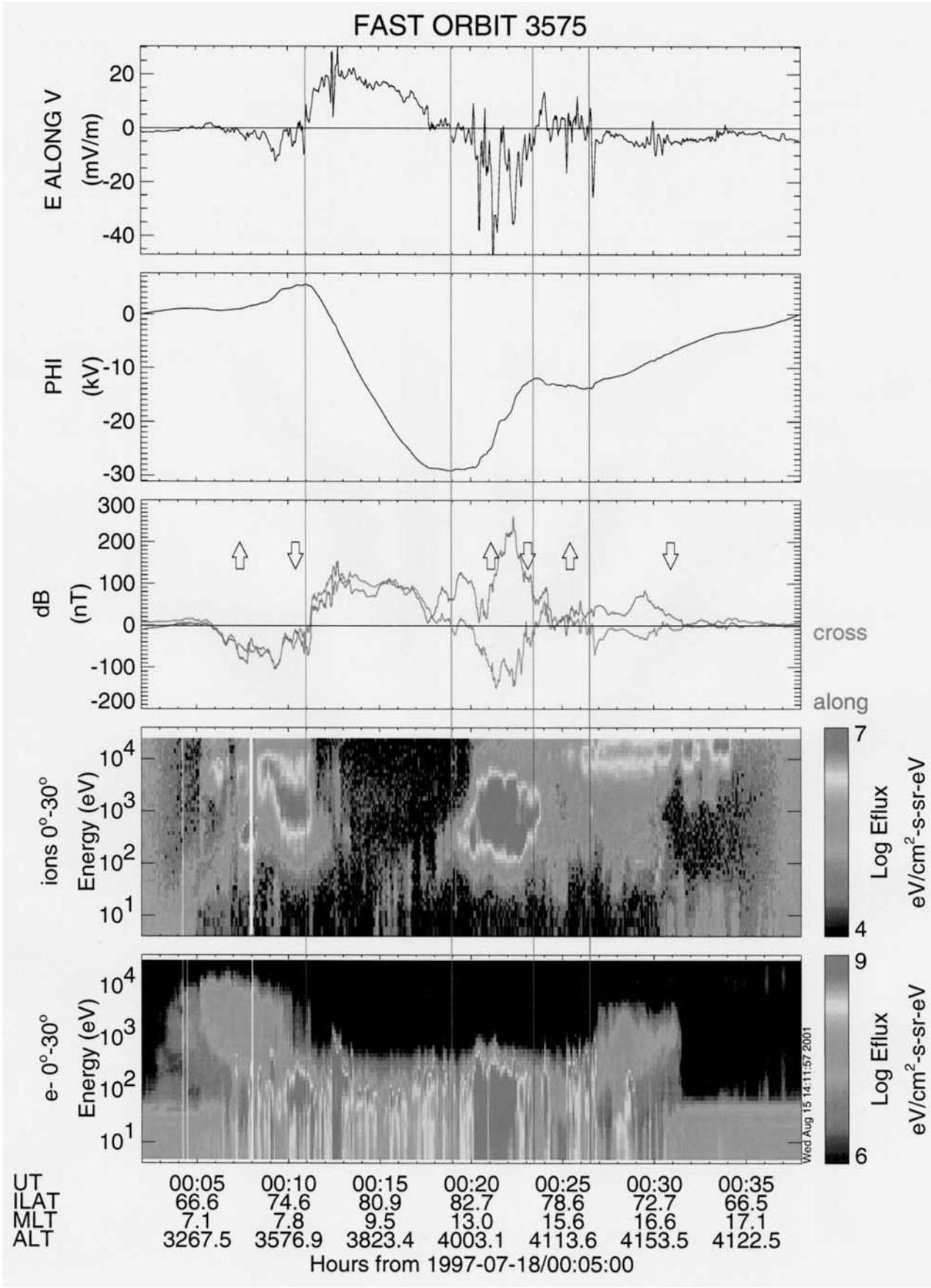

Figure 5. FAST orbit 3575. Same format as Figure 3. Four FACs are observed on the duskside for IMF B_y = 6.1 nT. See color version of this figure at back of this issue.

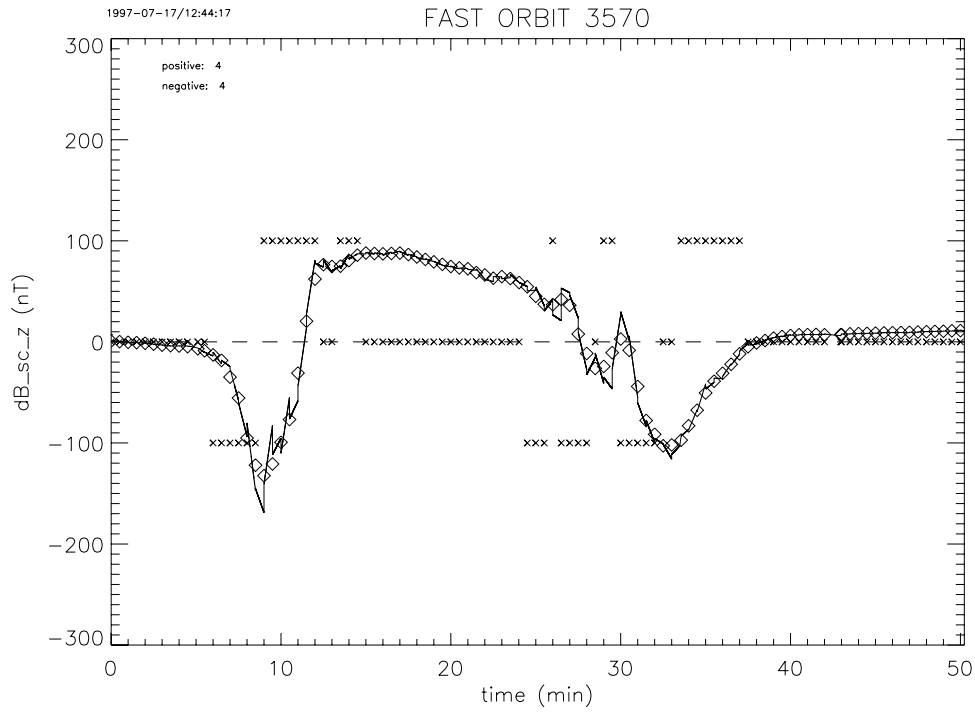

Figure 6. Pattern recognition result for FAST orbit 3570. Four upward and four downward current sheets were detected in dB_z, but only six FACs are considered as large-scale FACs. Four FACs are located on the duskside and two on the dawnside.

equatorward boundary of antisunward convection across the polar cap. The CRB is associated with a steep increase of ~45 mV/m in the electric field between 1322:30 and 1325:00 UT, after which the electric field shows a gradual increase by about 5 mV/m until 1330:00 UT. The steep slope in the electric field corresponds to a ~1050 km wide region of $\nabla \cdot \vec{E} > 0$ and an increase of ~250 nT in dB_z (downward current), while the gradual slope correlates with an additional increment of ~100 nT in dB_z until 1330:00 UT. Only sporadic low-energy electron precipitation is detected until 1325:00 UT whereas polar rain appear after 1325:00 UT. Ions of gradually lower energies characteristic of the plasma mantle [*Newell et al.*, 1991a] are observed in the downward current region as the satellite moves away from the CRB and further into the polar cap. Note that these mantle ions disappear after 1330:00 UT.

[23] The satellite finally traverses a pair of FACs with polarities and positions consistent with the duskside upward region 1 and downward region 2 current system. The poleward part of the region 1 current from 1334:30 to ~1336:00 UT coincides with a convection reversal from antisunward to sunward lower-latitude return flow in a region of $\nabla \cdot \vec{E} < 0$ and structured LLBL or BPS-like lower-energy electron precipitation. The equatorward part of this FAC from ~1336:00 to 1339:30 UT is characteristic of soft high-energy (>1 keV) BPS-like electron precipitation.

2.1.2. Event 2: 17 July 1997, 1250:00–1325:00 UT (FAST orbit 3570, $B_y > 0$)

[24] This event (Figures 4 and 6) is observed for an IMF (B_x, B_y, B_z) of (−3.1, 3.9, −1.6) nT and the large-scale potential drop across the polar cap is estimated to 60 kV.

[25] The large-scale electric field and dB_z perturbation magnetic field are well correlated also for this case. Two FACs appear in the dawnside auroral region, consistent with an upward region 2 current from 1251:00 UT and a downward region 1 current between 1253:05 and 1256:17 UT. The region 2 current is collocated with lower-latitude sunward flow and particle precipitation characteristic of the plasma sheet while the region 1 current is associated with a CRB from sunward to antisunward plasma convection across the polar cap. We note that structured lower-energy electron precipitation is detected mainly equatorward of the CRB in a region of smaller-scale electric and magnetic field variations. This population is found embedded in higher-energy BPS-like precipitating plasma.

[26] The duskside auroral region shows considerably more small-scale structure than the dawnside, in both fields and precipitating particles. The most striking feature is an electric field signature of antisunward and stagnant $\vec{E} \times \vec{B}$ convection within a much broader region of sunward plasma convection. The same general feature is detected in the dB_z perturbation magnetic field data. A similar electric field signature was seen in the previous example, but then observed on the dawnside. We will describe the observed duskside signature from lower to higher latitudes.

[27] A rather clear increase of ~115 nT is seen in dB_z from 1317:10 to 1321:40 UT and corresponds to a downward FAC in a region of sunward convection. The polarity and location are both consistent with a duskside region 2 current.

[28] A decrease of about 140 nT (upward current) is observed in dB_z from 1314:30 to 1317:10 UT on the poleward side of the region 2 current and coincides with a decrease in the electric field from positive to negative at lower latitudes, indicating a region of $\nabla \cdot \vec{E} < 0$. Electron precipitation detected in the poleward part of this upward

current is associated with structured electrons of increased energy flux in the approximate high-energy range from 550 eV to 2.0 keV and may be categorized as BPS or LLBL-like.

[29] The electric field just poleward of the upward current is associated with a steep positive gradient in a ~44 s wide (~250–300 km) region of $\nabla \cdot \vec{E} > 0$ between 1313:46 and 1314:30 UT. A simultaneous increase in dB_z of ~75 nT corresponds to a downward FAC. Note that electrons with energy above 20 eV are completely absent (unlike the observed electron precipitation of the dawnside region 1 current) and that the ion spectrogram indicates decreased energy flux below the background level of the lower-latitude BPS despite a downward directed current. Upflowing ionospheric electrons at energies below the instrument threshold carry the downward current (not shown). This region is not entirely void of ion precipitation, however. There is evidence of weaker ion energy flux above ~1 keV energy which seems to be associated with highly localized ion precipitation immediately poleward of the downward current.

[30] There are seven such ~15 s narrow (~70–100 km) ion precipitation signatures (between ~1309:30 and 1313:46 UT) poleward of the region of stagnant or antisunward convection. The three most equatorward features coincide with what appears to be sunward convection enhancements and display higher energy fluxes than the four most poleward ion signatures. A closer inspection of electron precipitation, superimposed smaller-scale magnetic field variations, and gradients in the electric field for all seven events show that electrons with average energies between 550 eV and 2.0 keV are detected in regions of intensified locally upward directed currents and associated with $\nabla \cdot \vec{E} < 0$ as was also observed by *Obara et al.* [1993]. The precipitating ions either coincide entirely with the location of electron precipitation, which is true for the two most poleward and the two most equatorward signatures, or are shifted somewhat poleward along the direction of the local average electric field. The large-scale electric field observed in conjunction with these particle events decreases gradually from positive (antisunward convection) over the polar cap, to a broader stagnation region of near zero electric field (from 1309:30 until 1311:30 UT) and precipitating ion signatures of much weaker energy flux, and finally turning strongly negative (sunward convection) where ions of comparably stronger energy flux are detected. The steep negative electric field gradient is collocated with a decreasing dB_z perturbation magnetic field which indicates an upward current in this region of LLBL-like precipitation [*Newell et al.*, 1991b]. In summary, we observe four FAC sheets on the duskside that coincide with the large-scale electric field signature of antisunward and stagnating sunward convection within a broader region of sunward convection equatorward of the polar cap CRB.

2.1.3. Event 3: 18 July 1997, 0002:00–0035:00 UT (FAST orbit 3575, $B_y > 0$)

[31] The good general agreement seen in the previous two cases between the along track component of the electric field and the cross-track magnetic perturbation field is again evident for this event (see Figure 5) with an observed IMF of (−2.1, 6.1, 1.2) nT. The peak-to-peak potential drop is about 35 kV.

[32] We interpret the dawnside negative and positive gradients in dB_z as an upward region 2 and downward region 1 current system. The region 2 current is collocated with plasma sheet-like ion and electron precipitation and a rather weak negative electric field which indicates a weakened sunward return flow in the magnetotail that may be related to the positive IMF B_z [*Wygant et al.*, 1983]. The downward region 1 current between 0009:15 and 0013:00 UT correlates well with a steep increase in the electric field and a CRB. Precipitating ions poleward of region 2, but equatorward of the CRB, shows a marked decrease in average energy that coincides with structured lower-energy electron precipitation embedded in a softer higher-energy BPS-like population. This region may be identified either as BPS or LLBL [*Newell et al.*, 1991b]. The part of region 1 which is located poleward of the CRB is mantle-like in character, despite the presence of electron acceleration events which is not an unusual observation in the plasma mantle as noted by *Newell et al.* [1991a].

[33] As in the previous example of positive IMF B_y, there is an electric field signature on the duskside of antisunward convection sandwiched between high-latitude and low-latitude sunward convection (red lines in Figure 5). The magnitude of the lower-latitude negative electric field is in qualitative agreement with the weak dawnside sunward return flow. We will again describe the data from low to high latitudes.

[34] There is a small increase of ~50 nT in dB_z between 0029:30 and 0034:20 UT which is collocated with plasma sheet-like particle precipitation and the weak sunward convection. We interpret this as a weak region 2 downward current.

[35] The average dB_z magnetic field immediately poleward of the region 2 current decreases gradually by about 80 nT between 0024:10 and 0029:30 UT. However, considering the observed particle precipitation and electric field, we may divide this large-scale upward current region in two parts of rather different character. The equatorward part coincides with weak sunward convection, smooth electric and magnetic fields, and high-energy electron precipitation that we identify as the dayside extension of the BPS. The poleward part is collocated with fluctuating magnetic and mostly positive electric fields (antisunward convection) that coincide with a sharp drop in electron average energy from soft high-energy BPS to structured low-energy LLBL-like electron precipitation. The negative excursion which is detected in both the electric and the dB_z magnetic fields near 0027:00 UT is associated with this particle boundary.

[36] A pair of much stronger oppositely directed FACs is observed poleward of the lower-latitude current system. We associate the region of strong and highly fluctuating sunward convection with this pair of balanced FACs and the downward FAC with its equatorward CRB. A noticeable ~120 s wide (~700 km) region of near stagnant convection (zero electric field) and near zero dB_z perturbation magnetic field exists on the poleward side of the region of sunward plasma convection. The strong upward current of the FAC pair is found in between this stagnation region and the downward FAC. Note that the east-west dB_z component of the magnetic field suggests an upward FAC even poleward of the stagnation region.

[37] Particle precipitation associated with the pair of strong FACs is characteristic of magnetosheath-like ions

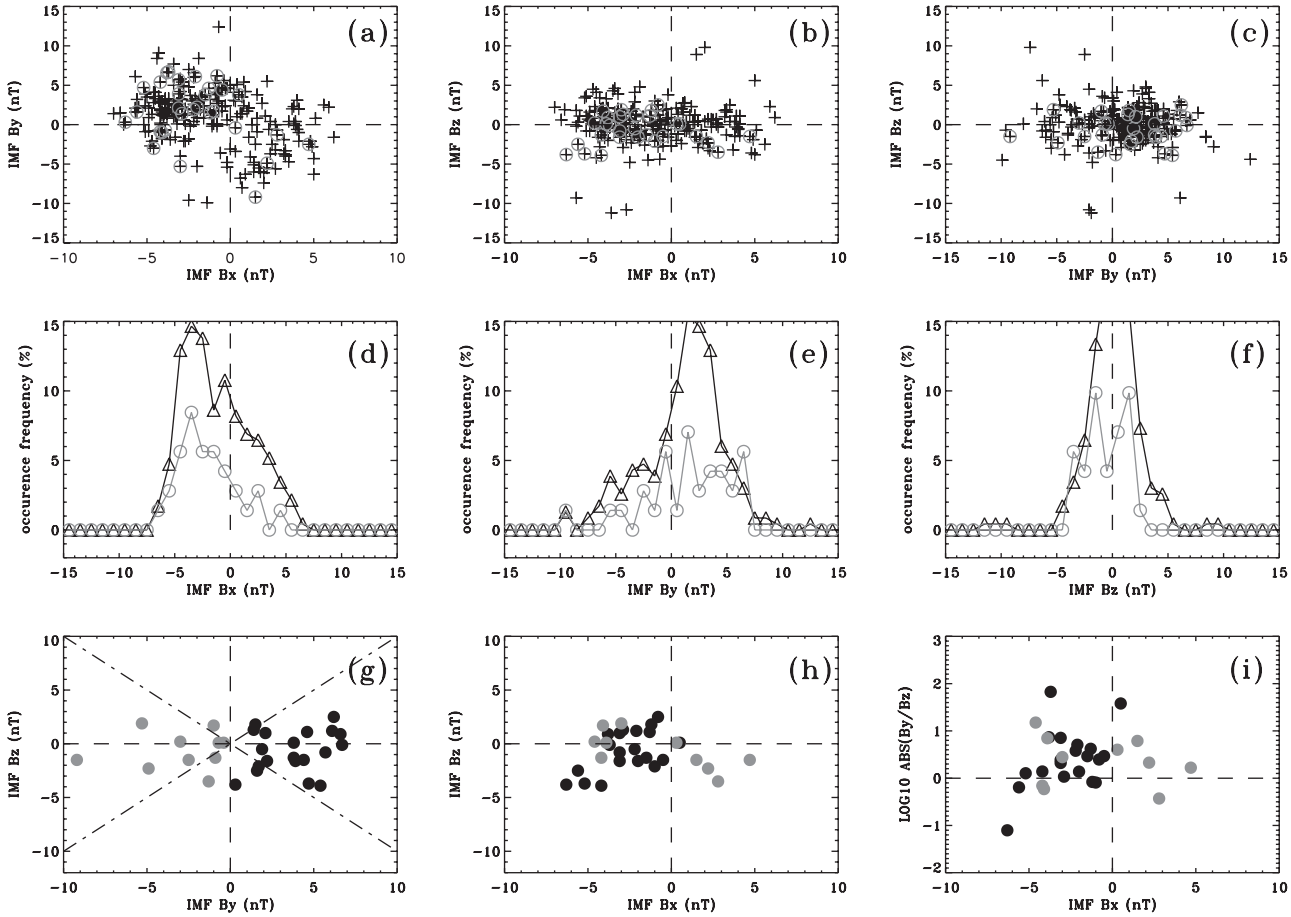

Figure 7. First row (a–c) shows IMF distribution of all 232 passes (black crosses) and the encircled 30 four FAC events (gray). Second row (d–f) shows the occurrence frequency versus IMF in 1 nT bins for two distributions; all 232 events (black triangle) and the 71 events for six FACs of alternating flow directions (gray circle). The last row (g–i) shows the IMF dependence for the 10 dawn events (gray) and the 20 dusk events (black) of four FAC events on either side of noon.

and electrons of high-energy fluxes with electron precipitation being concentrated to three sunward convection enhancements. Moreover, the increased ion energy flux is embedded in a softer BPS-like ion population that disappears abruptly at the poleward boundary of strong and erratic sunward convection. The mixed population of magnetosheath and BPS-like ions may be identified with the outer LLBL [*Newell et al.*, 1991b]. Lower-energy ion precipitation within and poleward of the stagnation region correspond to the plasma mantle [*Newell et al.*, 1991a].

[38] We have described three examples of an electric field signature that successively displays sunward, antisunward, sunward, and antisunward convection with latitude. It is associated with a current system of four FACs. The position of this electromagnetic structure was seen to shift from one side of the noon-midnight meridian to the other in response to the dawn-dusk (B_y) component of the IMF. The following subsection examines this apparent IMF positional dependence statistically for a total of 30 cases in July 1997.

2.2. Statistical Results

[39] A manual inspection of all events showing between six and eight FACs detected by the automated FAC algorithm resulted in 71 cases of six FACs with alternating upward and downward directed currents along the dawn-dusk orbit. A total of 30 cases from that set displayed a signature of four FACs either completely on the dawnside or the duskside, while the remaining 41 cases showed three FACs on each side of the noon midnight meridian. The IMF distribution for all 232 analyzed events and the subset of 30 four FAC events are shown in Figures 7a–7c as black crosses and gray circles respectively. The second row (Figures 7d–7f) shows the occurrence frequency versus IMF in 1 nT bins for two distributions, a black triangle for the 232 events and a gray circle for all 71 events with six large-scale FACs. Note that the IMF for all 232 FAST passes display the typical garden-hose or Parker spiral distribution [*Ness and Wilcox*, 1964]. IMF is most often directed duskward and antisunward in July 1997, rather than dawnward and sunward (see Figures 7a and 7d–7e). The IMF for the 71 events of six large-scale FACs display a similar distribution, but with a larger degree of statistical fluctuation. The last row illustrates the subset of 30 events versus IMF. A gray dot indicates that four FACs are found on the dawnside and a black dot for those found on the duskside (Figure 7g). Note the clear IMF B_y dependence of the spatial location for the system of four FACs with dawnside events for $B_y < 0$ and duskside events occurring

Table 1. Interplanetary Magnetic Field Dependence of Four Field-Aligned Current Sheets Found Either on the Dawn or the Duskside for a Subset of 30 Events

	$\|B_y/B_z\| < 1$	$\|B_y/B_z\| > 1$
$B_x > 0$	1	5
$B_x < 0$	6	18

for $B_y > 0$. Figure 7h indicates that most duskside events for $B_y > 0$ occur for $B_x < 0$ as would be expected from the Parker spiral. However, only 50% of the 10 dawnside events for $B_y < 0$ occur for $B_x > 0$. The dependence of four FACs on IMF B_x and the ratio $|B_y/B_z|$ as displayed in Figure 7i is summarized in Table 1. A majority of the 30 events thus indicates the importance of either having $|B_y/B_z| > 1$ (23 cases) or $B_x < 0$ (24 cases). Such a dependence upon IMF configuration suggests that the additional structure in convection and FACs results from a reconnection-driven process. In particular, it suggests a reconnection site on the tail magnetopause between the magnetosheath and lobe magnetic fields, where the lobe field is dominated by its x and y components, such as that observed on ISEE 2 [*Gosling et al.*, 1991].

[40] Figures 8 and 9 show the midpoint of each FAC in ILat versus magnetic local time (MLT) for the 10 dawnside events and the 20 duskside events respectively. The corresponding IMF is presented as well. The highest-latitude FAC occasionally ranges over longer distances along the satellite track than the three equatorward FACs observed as a system of four adjacent current sheets. This is why it is sometimes found farther away from the other FACs in Figures 8 and 9. We observe that the four large-scale FACs described in Figures 3–5 (orbits 3462, 3570, and 3575) are located more than three hours from 1200 MLT. The occurrence of the additional FACs far from noon is common in our sample (20 cases out of 30), and indicates that these FAC systems and the convection that they support extend across the entire dayside, as was suggested by *Ohtani and Higuchi* [2000], rather than being localized to regions near the noon and cusp [*Taguchi et al.*, 1993].

3. Discussion

[41] In summary, observations of electric and perturbation magnetic fields imply a region of antisunward or stagnant convection within a typically broader region of sunward convection which is detected either on the dawnside or the duskside depending on IMF B_y. The region of antisunward and lower-latitude sunward convection coincides with a FAC of the same direction as a region 1 current adjacent to the region 2 current. We interpret this electric field signature in terms of the so-called viscous cell [e.g., *Burch et al.*, 1985; *Reiff and Luhmann*, 1986; *Siscoe et al.*, 1991].

[42] Moving poleward into the polar cap, we observe a pair of oppositely directed large-scale gradients in the cross-track perturbation magnetic field poleward of the region 1 current. The equatorward current sheet is oppositely directed to the adjacent region 1 current and coincides with a plasma flow reversal from the antisunward part of the viscous cell to a broader region of fluctuating sunward convection which is interpreted as the lower-latitude part of a lobe cell [e.g., *Burch et al.*, 1985; *Crooker et al.*, 1998]. FAST encountered a third CRB inside the assumed lobe cell which at times displays a clear stagnation signature (see Figure 5). The equatorward part of the highest-latitude current sheet is associated with this CRB.

[43] When comparing the signature of four adjacent FACs for $B_y < 0$ with the MHD model results of *Ogino et al.* [1986] we note that the FACs referred to as polar cap currents in their Figure 2 agree rather well with what FAST observes poleward of the region 1 current from 6 to 12 MLT (see Figure 8). We shall for sake of simplicity refer to the highest-latitude pair of opposite FACs as the lobe current system after its close connection with the dawnward electric field signature of a lobe reconnection mechanism. The

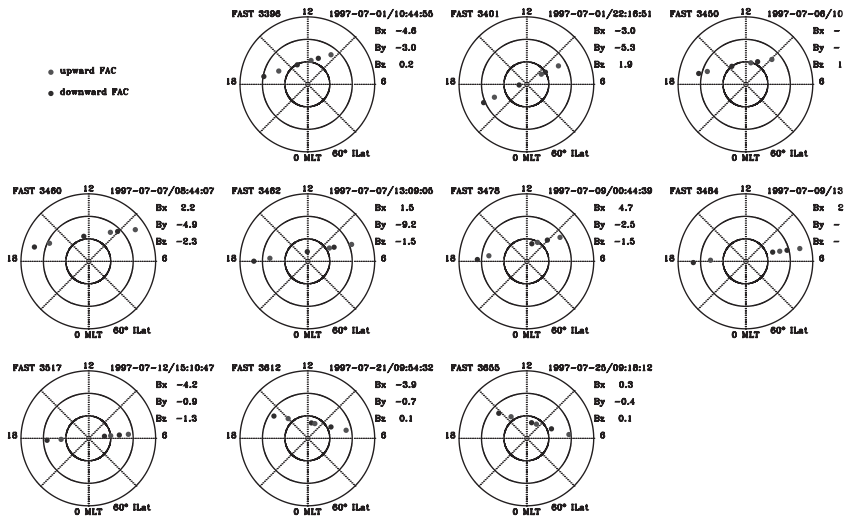

Figure 8. All 10 dawnside events with each large-scale FAC indicated in invariant latitude (ILat) versus magnetic local time (MLT). A gray dot shows the midlocation of an upward current region and the black dot shows a downward FAC. The time (UT) when FAST passes 50° ILat (poleward-bound) and the corresponding IMF from Wind are indicated on the righthand side.

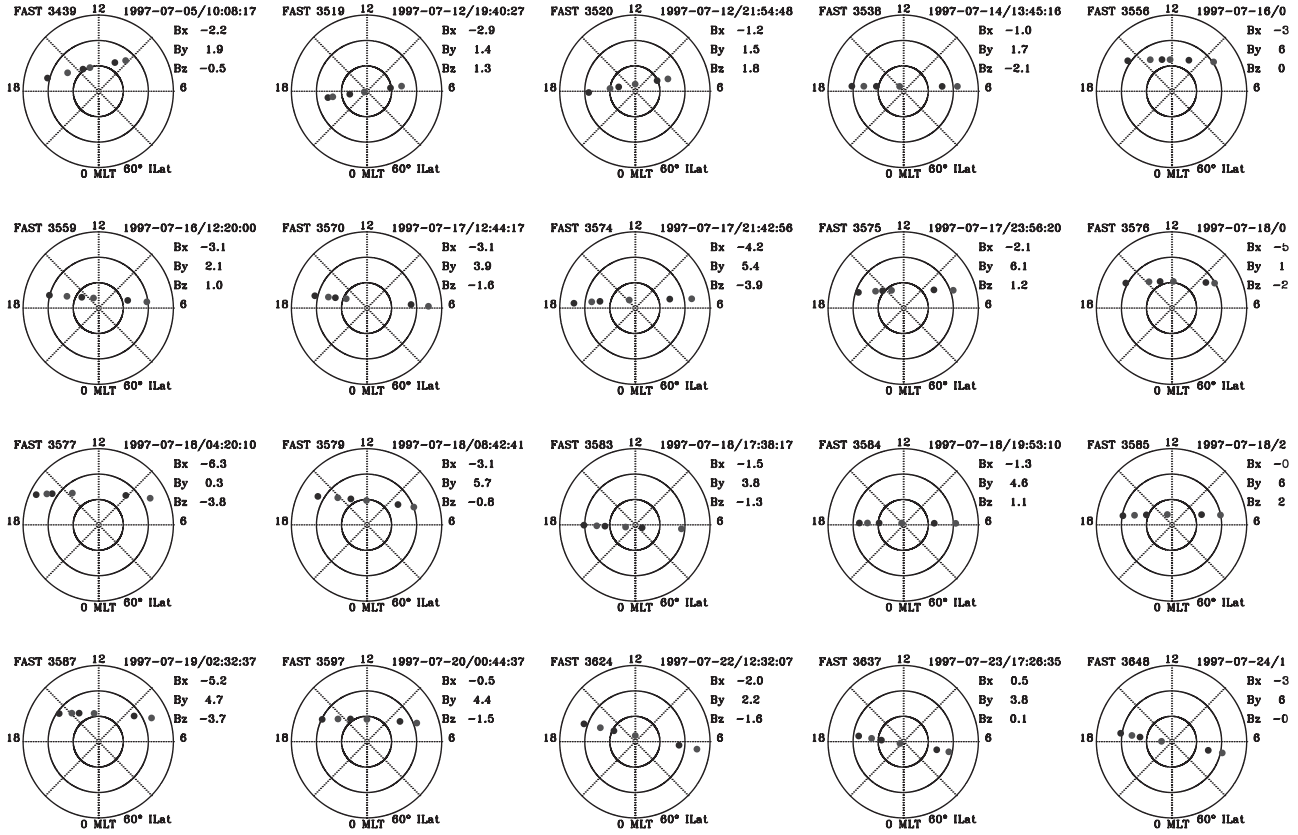

Figure 9. All 20 duskside events with each large-scale FAC indicated in ILat versus MLT. Same format as Figure 8.

dawnward electric field signifies sunward convection near the dawn and dusk polar cap edges (see Figure 10b below).

[44] Seemingly independent of B_y, particle precipitation in the upward lobe current consists either of electrons and ions of magnetosheath-like energies similar to cusp ~1 keV ion injections observed near noon mixed with BPS-like ion precipitation (see Figure 5) or is identified with the LLBL of approximately 600 eV to 2.5 keV electrons and $\geq$2 keV ions (see Figures 3 and 4). A mixed population of stagnant (as opposed to tailward flowing) magnetosheath-plasma sheet ions similar to what is observed here (Figure 5) was detected by the Wind spacecraft deep inside the magnetotail lobes [*Phan et al.*, 2000] in the approximate region of $-7R_E < x_{GSM} < -3R_E$.

[45] Moreover, the cusp-like particles precipitate in a region of sunward convection, not antisunward as would be expected for cusp injections due to dayside subsolar magnetopause merging with the IMF. We interpret this type of injection as due to lobe reconnection poleward of the cusp [e.g., *Matsuoka et al.*, 1996] in a region where the geomagnetic field is predominantly in the dawnward or the duskward direction [*Reiff and Burch*, 1985]. Electron precipitation is further associated with sunward convection enhancements, as would be expected for localized multiple reconnection on the lobe magnetopause flanks. Patchy ion precipitation of plasma sheet-like energies on embedded smaller scale upward FACs was observed in one case to occur close to such enhancements (see Figure 4), but shifted somewhat poleward along the direction of the local electric field as compared with the electrons.

[46] The question is how BPS or LLBL-like electrons and ions may precipitate on upward currents of newly opened field lines associated with a merging process. *Siscoe and Sanchez* [1987] suggested that component merging primarily of the IMF B_y with the nightside lobe magnetic field of the high-latitude boundary layer creates a relatively thin layer of rotational discontinuity in the *yz* plane of the plasma mantle that would produce a FAC on open field lines. These currents have the same polarity as the region 1 current and may correspond to the higher-latitude lobe current (or its poleward part) observed by FAST. They further proposed that these tail-aligned currents may drive a secondary circulation in the *yz* plane of the magnetotail that would bring plasma from the plasma sheet and the LLBL up along the duskside (dawnside) flanks of the tail for positive (negative) B_y. The MHD model by *Ogino et al.* [1986] resulted in the same IMF B_y-dependent twist of the plasma sheet and LLBL. *Siscoe and Sanchez* [1987] seem to imply a localized region of antiparallel reconnection between the plasma mantle and the LLBL which they termed the juncture point, but did not mention this possibility explicitly.

[47] We have reproduced the proposed twist of the cross-tail plasma sheet in Figure 10a for $B_y > 0$, $B_z < 0$, and $B_x < 0$. The juncture point or juncture line is indicated between the two arrows and the *x* component of magnetospheric convection is shown as well. Assuming an antiparallel lobe reconnection site at the juncture between the plasma mantle (rotational discontinuity) and the LLBL (tangential discontinuity) that creates earthward accelerated flows of plasma under the assumption that the local Alfvén velocity is larger

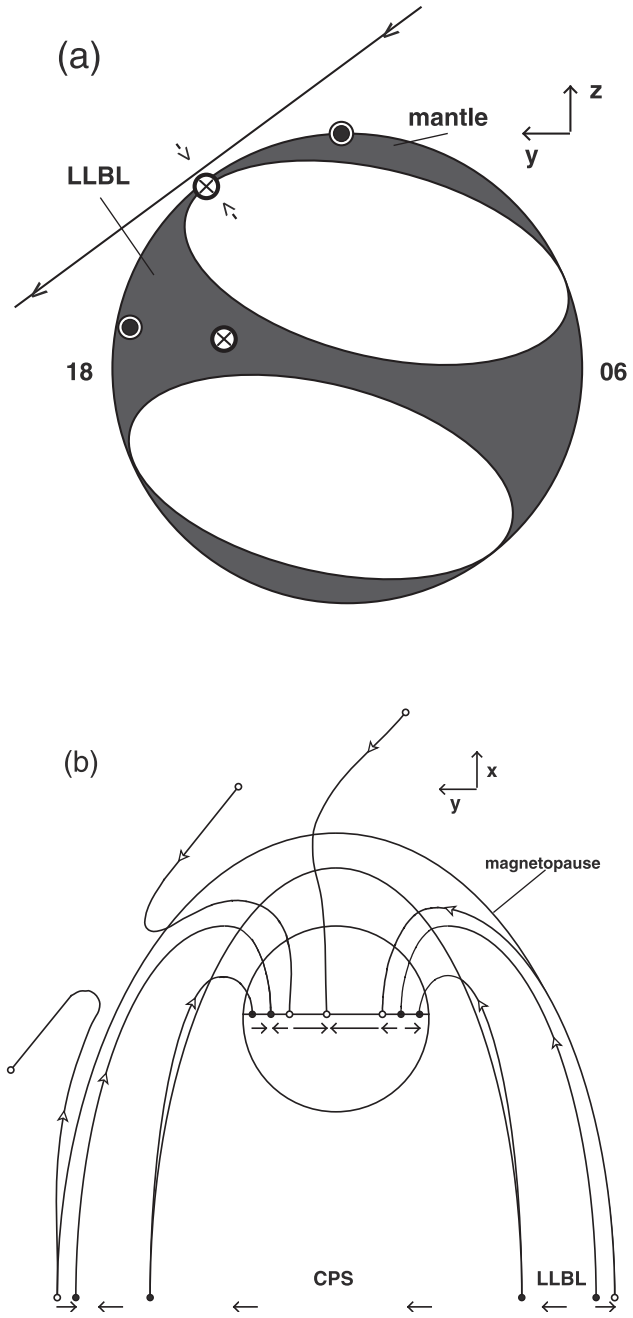

Figure 10. (a) A sketch of the twist induced in the location of the plasma sheet and LLBL by a positive IMF B_y component (reproduced after *Siscoe and Sanchez* [1987]) and (b) a sketch of its equatorial projection for lobe reconnection in the duskside juncture region. The magnetic field is indicated by open arrows and shown in three dimensions. The open or closed nature of its foot points is shown as open or solid circles. The directions of the corresponding electric fields are indicated by arrows.

than the speed of the magnetosheath flow could explain the precipitation of BPS and LLBL-like ions and electrons in the upward lobe current region on sunward convecting plasma. This situation may be fulfilled in the slow-mode shock region tailward of the dawn-dusk meridan plane [*Siscoe and Sanchez*, 1987]. Figure 10b illustrates the schematic projection of the magnetosphere onto the equatorial *xy* plane for the merging configuration in Figure 10a. The direction of the magnetic field in the Northern Hemisphere is marked with open arrows and its open or closed field line character is indicated by an open or closed circle at the foot points. The electric field and perturbation magnetic field associated with each magnetospheric region are assumed to map along equipotential magnetic field lines to the ionosphere. Lobe reconnection in the duskside flank magnetopause region produces a wedge of sunward convection equatorward of polar cap antisunward convection but poleward of antisunward flow of the outer LLBL consistent with the ionospheric observations made in this study.

[48] Precipitation in the downward lobe current region of the poleward pair of FACs is expected to be dependent on whether B_y is negative or positive, thus generating a current sheet poleward (on the dawnside) or equatorward (on the duskside) of the upward lobe current. If located on the equatorward side, it is probably generated in a velocity shear region between antisunward convection of the lower-latitude viscous cell and sunward convection of the higher-latitude lobe cell. In this case it may be considered a secondary effect to the lobe reconnection driven upward current. Particle precipitation should thus be characteristic of the LLBL or BPS (Figures 4 and 5). If located on the poleward side of the upward FAC, the current generator is probably associated with a rotational discontinuity on open field lines between the magnetosheath magnetic field and the lobe magnetic field [*Siscoe and Sanchez*, 1987]. Particle precipitation should then to a greater extent be characteristic of low-energy plasma from the mantle, as was observed for ions in the case of negative IMF B_y presented here (Figure 3). It is possible that the upward FAC detected poleward of the stagnation region of the lobe cell (Figure 5) is associated with this current generation mechanism.

[49] The distribution of IMF for 30 events of coincident four current sheets and global convection signatures, suggesting the simultaneous presence of lobe cells and viscous-type of cells, clearly indicates that a majority of events occur for southward IMF conditions ($B_z < 2$ nT) and $|B_y/B_z| > 1$, consistent with the conclusion drawn by *Gosling et al.* [1991] that the importance of northward IMF for tail lobe reconnection in the Northern Hemisphere has been exaggerated.

[50] *Crooker and Rich* [1993] proposed that lobe cell convection is more likely to occur for summer conditions, since the flare angle of the tail lobe increases with dipole tilt. As a consequence, the probability of antiparallel alignment between the draped magnetosheath IMF and the summer hemisphere lobe field is increased. Summer conditions favor reconnection in the Northern Hemisphere for $B_x < 0$, and reconnection in the Southern Hemisphere for $B_x > 0$. Assuming a preferred garden-hose direction of the IMF, as was generally the case in July 1997, entails a positive (negative) B_y component when B_x is negative (positive). *Gosling et al.* [1986] found that duskside tail reconnection events were more common than dawnside events in a flank magnetopause survey of ISEE 1 and 2 data. However, the ISEE 1 and 2 spacecraft sampled the dawnside region to a lesser extent than the duskside due to

the orbital plane of the spacecraft, making interpretations of the dawn-dusk asymmetry and its possible connection with the results of *Crooker and Rich* [1993] difficult. The dawn-dusk asymmetry is suggested in the statistics provided here (see Figures 7g–7i) with 20 duskside events for $B_y > 0$ and mostly $B_x < 0$, while only 10 dawnside events are detected for $B_y < 0$. Furthermore, B_x is negative for five of the dawnside cases, thus belonging to a less probable IMF configuration, but consistent with lobe reconnection for summer conditions [*Crooker and Rich*, 1993]. The five remaining dawnside cases occur for positive B_x and belong to the more probable IMF category. These cases are inconsistent though with lobe reconnection in the Northern Hemisphere for summer conditions if the B_x component alone is of importance for merging. However, there is a tendency of IMF $|B_y/B_z| > 1$ for the dawnside cases of positive B_x. This suggests the significance of the IMF B_y component for merging with the lobe magnetic field at the dawnside flank, where the x and y components of the magnetospheric field dominate. The dawn-dusk asymmetry in favor of duskside lobe convection events thus seems to originate as a combined effect of IMF garden-hose angle and the preference of oppositely directed IMF B_x and lobe geomagnetic field.

[51] What seems to be of importance for the occurrence of lobe cell convection near the auroral oval edges and the associated signature of four FACs are the B_x component of the IMF and the ratio $|B_y/B_z|$. Note also that most FAST passes in July 1997 occurred for IMF $|B_y| \leq 5$ nT. If we had applied the IMF criteria of *Taguchi et al.* [1993], we would have missed 21 out of 30 events. Whether or not so-called cleft particles are observed seems to depend on the strength of the electric field associated with sunward convection enhancements, assumed to originate from localized near-tail flank reconnection.

4. Conclusions

[52] We have analyzed the occurrence and distribution of four field-aligned currents for one month's worth of data near summer solstice in the Northern Hemisphere. Evidence of ionospheric lobe cell convection coinciding with a pair of Birkeland currents poleward of the region 1 current is presented using simultaneous magnetic field, electric field, and precipitating particle data. The statistical results can be summarized as follows:

1. A total number of 71 cases (~30%), indicating six FACs of alternating polarity along the satellite track, remain after manual inspection of events suggesting between six and eight FACs. A subset of 30 events display four FACs on one side of the noon-midnight meridian and two FACs on the opposite side. The lowest-latitude pair of current sheets are interpreted as a region 1 and region 2 current system. The current flow directions of the additional pair of FACs poleward of the region 1 current are consistent with the polar cap current distribution of *Ogino et al.* [1986].

2. All 30 events occur for $-3.9 \leq B_z \leq 2.5$ nT, the average B_z being -0.7 nT. A total of 13 events occur for $B_z > 0$. Only two of these occur for $B_x > 0$. Thus we find no preference for lobe cells to occur for northward IMF as was originally proposed by *Russell* [1972] and recently suggested by *Ohtani and Higuchi* [2000].

3. Twenty events show four current sheets on the duskside for $B_y > 0$ with an average B_y of 3.7 nT. B_x = 0.5 nT for the single event being positive.

4. Ten events show four current sheets on the dawnside for $B_y < 0$ with an average B_y of -2.9 nT. Despite the prefered garden-hose direction of the IMF ($B_x > 0$), 50% of these events occurred for $B_x < 0$. On the other hand, four out of five events for $B_x > 0$ show a ratio of $|B_y/B_z| > 1$.

5. The IMF $|B_y/B_z|$ ratio and the direction of B_x both seem important for the occurrence of the pair of Birkeland currents poleward of the region 1 current. 18 events have $B_x < 0$ and a ratio larger than one, while only six events occurred for a ratio less than one and $B_x < 0$. Five events had a positive B_x, but a ratio larger than one.

6. The results from this combined case and statistical study are consistent with a model of global convection in the ionosphere of coexisting dayside merging, lobe cell, and viscous-type of cells [*Burch et al.*, 1985; *Reiff and Burch*, 1985]. The observations further support the hypothesis that lobe cell convection is driven by merging occuring on the high-latitude flank or lobe magnetopause simultaneous to the merging on the low-latitude dayside magnetopause that drives the merging cells of the standard two-cell convection pattern.

7. A dawn-dusk asymmetry is present in favor of duskside lobe cells which we propose is due to a combination of the Parker spiral and the higher probability for tail lobe reconnection to occur for $B_x < 0$ in the Northern Hemisphere during summer conditions.

[53] We propose that four large-scale field-aligned currents appear over a wider local time than was suggested by *Ohtani et al.* [1995b] as a result of coinciding lobe reconnection and lower-latitude viscous-like convection. The present study also suggests that the upward FAC detected poleward of the region 1 current is generated in a localized antiparallel reconnection region in the near-tail flanks independent of IMF B_y. The downward FAC located poleward of the region 1 may be generated as a consequence of a rotational discontinuity on open field lines ($B_y < 0$) or generated in a region of sheared plasma convection between the lower-latitude antisunward flow of the LLBL and the higher-latitude sunward flow of the lobe cell ($B_y > 0$).

[54] Further studies of the magnetic local time distribution of four FACs and the associated particle precipitation in both hemispheres may shed further light on the signatures of lobe reconnection in the ionosphere and its seasonal dependence.

[55] **Acknowledgments.** S.E. thanks Tomas Karlsson and Robert J. Strangeway for useful discussions and the SPRG of UC Berkeley for making the FAST and Wind data sets available.

[56] Michel Blanc thanks George Siscoe and another referee for their assistance in evaluating this paper.

References

Burch, J. L., P. H. Reiff, J. D. Menietti, R. A. Heelis, W. B. Hanson, S. D. Shawhan, E. G. Shelley, M. Sugiura, D. R. Weimer, and J. D. Winningham, IMF B_y-dependent plasma flow and Birkeland currents in the dayside magnetosphere, 1, Dynamics Explorer observations, *J. Geophys. Res.*, *90*, 1577–1593, 1985.

Bythrow, P. F., T. A. Potemra, L. J. Zanetti, R. A. Erlandson, D. A. Hardy, F. J. Rich, and M. H. Acuna, High latitude currents in the 0600 to 0900 MLT sector: Observations from Viking and DMSP-F7, *Geophys. Res. Lett.*, *14*, 423–426, 1987.

Bythrow, P. F., T. A. Potemra, R. E. Erlandson, and L. J. Zanetti, Birkeland currents and charged particles in the high-latitude prenoon region: A new interpretation, *J. Geophys. Res.*, *93*, 9791–9803, 1988.

Carlson, C. W., R. F. Pfaff, and J. G. Watzin, The Fast Auroral SnapshoT (FAST) mission, *Geophys. Res. Lett.*, *25*, 2013–2016, 1998.

Cattell, C., R. Lysak, R. B. Torbert, and F. S. Mozer, Observations of differences between regions of current flowing into and out of the ionosphere, *Geophys. Res. Lett.*, *6*, 621–624, 1979.

Crooker, N. U., and F. J. Rich, Lobe cell convection as a summer phenomenon, *J. Geophys. Res.*, *98*, 13,403–13,407, 1993.

Crooker, N. U., J. G. Lyon, and J. A. Fedder, MHD model merging with IMF B_y: Lobe cells, sunward polar cap convection, and overdraped lobes, *J. Geophys. Res.*, *103*, 9143–9151, 1998.

Eriksson, S., R. E. Ergun, C. W. Carlson, and W. Peria, The cross-polar potential drop and its correlation to the solar wind, *J. Geophys. Res.*, *105*, 18,639–18,653, 2000.

Gosling, J. T., M. F. Thomsen, S. J. Bame, and C. T. Russell, Accelerated plasma flows at the near-tail magnetopause, *J. Geophys. Res.*, *91*, 3029–3041, 1986.

Gosling, J. T., M. F. Thomsen, S. J. Bame, R. C. Elphic, and C. T. Russell, Observations of reconnection of interplanetary and lobe magnetic field lines at the high-latitude magnetopause, *J. Geophys. Res.*, *96*, 14,097–14,106, 1991.

Gosling, J. T., M. F. Thomsen, G. Le, and C. T. Russell, Observations of magnetic reconnection at the lobe magnetopause, *J. Geophys. Res.*, *101*, 24,765–24,773, 1996.

Heikkila, W. J., Magnetospheric topology of fields and currents, in *Magnetospheric Currents*, *Geophys. Monogr. Ser.*, vol. 28, edited by T. A. Potemra, pp. 208–222, AGU, Washington, D. C., 1984.

Iijima, T., and T. A. Potemra, Field-aligned currents in the dayside cusp observed by Triad, *J. Geophys. Res.*, *81*, 5971–5979, 1976.

Iijima, T., R. Fujii, T. A. Potemra, and N. A. Saflekos, Field-aligned currents in the south polar cusp and their relationship to the interplanetary magnetic field, *J. Geophys. Res.*, *83*, 5595–5603, 1978.

Marklund, G. T., L. G. Blomberg, C.-G. Fälthammar, R. E. Erlandson, and T. A. Potemra, Signatures of the high-altitude polar cusp and dayside auroral regions as seen by the Viking electric field experiment, *J. Geophys. Res.*, *95*, 5767–5780, 1990.

Matsuoka, A., K. Tsuruda, H. Hayakawa, T. Mukai, and A. Nishida, Electric field structure and ion precipitation in the polar region associated with northward interplanetary magnetic field, *J. Geophys. Res.*, *101*, 10,711–10,736, 1996.

McDiarmid, I. B., J. R. Burrows, and M. D. Wilson, Comparison of magnetic field perturbations at high latitudes with charged particle and IMF measurements, *J. Geophys. Res.*, *83*, 681–688, 1978.

Ness, N. F., and J. M. Wilcox, Solar origin of the interplanetary magnetic field, *Phys. Rev. Lett.*, *13*, 461–464, 1964.

Newell, P. T., W. J. Burke, C.-I. Meng, E. R. Sanchez, and M. E. Greenspan, Identification and observation of the plasma mantle at low altitude, *J. Geophys. Res.*, *96*, 35–45, 1991a.

Newell, P. T., W. J. Burke, E. R. Sanchez, C.-I. Meng, M. E. Greenspan, and C. R. Clauer, The low-latitude boundary layer and the boundary plasma sheet at low altitude: Prenoon precipitation regions and convection reversal boundaries, *J. Geophys. Res.*, *96*, 21,013–21,023, 1991b.

Obara, T., T. Mukai, H. Hayakawa, A. Nishida, K. Tsuruda, S. Machida, and H. Fukunishi, Akebono (EXOS D) observations of small-scale electromagnetic signatures relating to polar cap precipitation, *J. Geophys. Res.*, *98*, 11,153–11,159, 1993.

Ogino, T., R. J. Walker, M. Ashour-Abdalla, and J. M. Dawson, An MHD simulation of the effects of the interplanetary magnetic field B_y component on the interaction of the solar wind with the Earth's magnetosphere during southward interplanetary magnetic field, *J. Geophys. Res.*, *91*, 10,029–10,045, 1986.

Ohtani, S., and T. Higuchi, Four-sheet structures of dayside field-aligned currents: Statistical study, *J. Geophys. Res.*, *105*, 25,317–25,324, 2000.

Ohtani, S., T. A. Potemra, P. T. Newell, L. J. Zanetti, T. Iijima, M. Watanabe, M. Yamauchi, R. D. Elphinstone, O. de la Beaujardière, and L. G. Blomberg, Simultaneous prenoon and postnoon observations of three field-aligned current systems from Viking and DMSP-F7, *J. Geophys. Res.*, *100*, 119–136, 1995a.

Ohtani, S., T. A. Potemra, P. T. Newell, L. J. Zanetti, T. Iijima, M. Watanabe, L. G. Blomberg, R. D. Elphinstone, J. S. Murphree, M. Yamauchi, and J. G. Woch, Four large-scale field-aligned current systems in the dayside high-latitude region, *J. Geophys. Res.*, *100*, 137–153, 1995b.

Phan, T. D., R. P. Lin, S. A. Fuselier, and M. Fujimoto, Wind observations of mixed magnetosheath-plasma sheet ions deep inside the magnetosphere, *J. Geophys. Res.*, *105*, 5497–5505, 2000.

Phan, T. D., B. U. Ö. Sonnerup, and R. P. Lin, Fluid and kinetics signatures of reconnection at the dawn tail magnetopause: Wind observations, *J. Geophys. Res.*, *106*, 25,489–25,501, 2001.

Reiff, P. H., and J. L. Burch, IMF B_y-dependent plasma flow and Birkeland currents in the dayside magnetosphere, 2, A global model for northward and southward IMF, *J. Geophys. Res.*, *90*, 1595–1609, 1985.

Reiff, P. H., and J. G. Luhmann, Solar wind control of the polar-cap voltage, in *Solar Wind-Magnetosphere Coupling*, edited by Y. Kamide and J. A. Slavin, pp. 453–476, Terra Sci., Tokyo, 1986.

Russell, C. T., The configuration of the magnetosphere, in *Critical Problems of Magnetospheric Physics*, edited by E. R. Dyer Jr., pp. 1–16, Natl. Acad. Sci., Washington, D. C., 1972.

Sanchez, E. R., G. L. Siscoe, and C.-I. Meng, Inductive attenuation of the transpolar voltage, *Geophys. Res. Lett.*, *18*, 1173–1176, 1991.

Siscoe, G. L., and E. Sanchez, An MHD model for the complete open magnetotail boundary, *J. Geophys. Res.*, *92*, 7405–7412, 1987.

Siscoe, G. L., W. Lotko, and B. U. Ö. Sonnerup, A high-latitude, low-latitude boundary layer model of the convection current system, *J. Geophys. Res.*, *96*, 3487–3495, 1991.

Sugiura, M., N. C. Maynard, W. H. Farthing, J. P. Heppner, B. G. Ledley, and L. J. Cahill Jr., Initial results on the correlation between the magnetic and electric fields observed from the DE-2 satellite in the field-aligned current regions, *Geophys. Res. Lett.*, *9*, 985–988, 1982.

Taguchi, S., M. Sugiura, J. D. Winningham, and J. D. Slavin, Characterization of the IMF B_y-dependent field-aligned currents in the cleft region based on DE 2 observations, *J. Geophys. Res.*, *98*, 1393–1407, 1993.

Wygant, J. R., R. B. Torbert, and F. S. Mozer, Comparison of S3-3 polar cap potential drops with the interplanetary magnetic field and models of magnetopause reconnection, *J. Geophys. Res.*, *88*, 5727–5735, 1983.

Zanetti, L. J., and T. A. Potemra, Correlated Birkeland current signatures from the Triad and Magsat magnetic field data, *Geophys. Res. Lett.*, *9*, 349–352, 1982.

J. W. Bonnell and C. W. Carlson, Space Sciences Laboratory, University of California, Berkeley, CA 94720-7450, USA. (jbonnell@ssl.berkeley.edu; cwc@ssl.berkeley.edu)

R. E. Ergun, Department of Astrophysical and Planetary Science, Laboratory for Atmospheric and Space Physics, University of Colorado, Boulder, Box 590, Boulder, CO 80309, USA. (ree@fast.colorado.edu)

S. Eriksson, L. G. Blomberg, and G. T. Marklund, Alfvén Laboratory, Royal Institute of Technology, SE-10044, Stockholm, Sweden. (eriksson@plasma.kth.se; blomberg@plasma.kth.se; marklund@plasma.kth.se)

Figure 3. (opposite) FAST orbit 3462. The panels display (from top to bottom): the along-track electric field and electric potential (assuming return to zero potential at low latitudes), the cross-track dB_z (green) and along-track dB_y (red) perturbation magnetic fields in a spacecraft coordinate system, and the precipitating ions and electrons, respectively. A green vertical line marks the maximum and minimum electric potential. A red line marks any CRB equatorward of these. Four FACs are observed on the dawnside for IMF $B_y = -9.2$ nT.

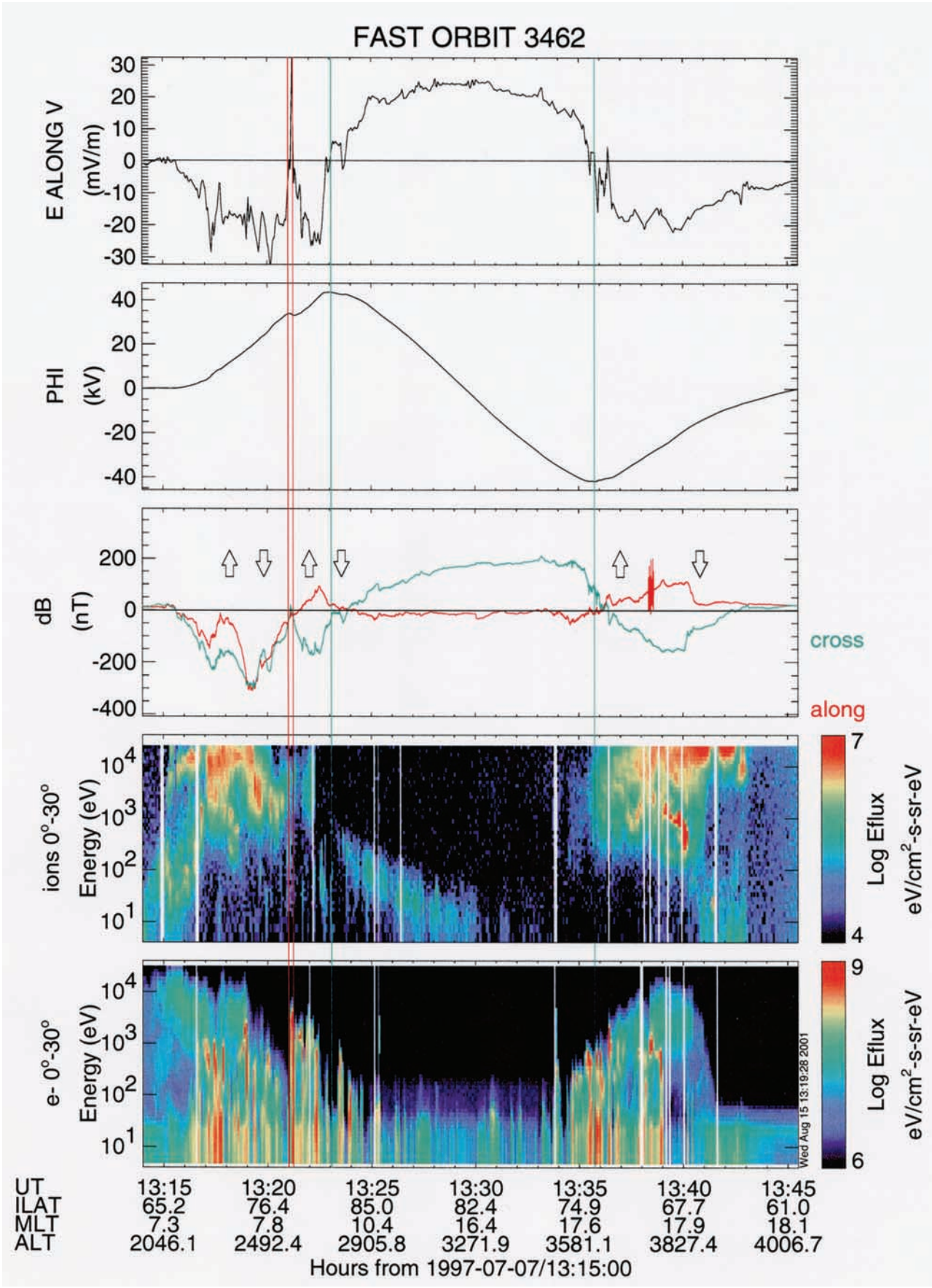
FAST ORBIT 3462
E ALONG V
(mV/m)
30
20
10
0
-10
-20
-30
PHI
(kV)
40
20
0
-20
-40
dB
(nT)
200
0
-200
-400
cross
along
ions 0°-30°
Energy (eV)
10^4
10^3
10^2
10^1
Log Eflux
eV/cm^2-s-sr-eV
7
4
e- 0°-30°
Energy (eV)
10^4
10^3
10^2
10^1
Log Eflux
eV/cm^2-s-sr-eV
9
6
Wed Aug 15 13:19:28 2001
UT 13:15 13:20 13:25 13:30 13:35 13:40 13:45
ILAT 65.2 76.4 85.0 82.4 74.9 67.7 61.0
MLT 7.3 7.8 10.4 16.4 17.6 17.9 18.1
ALT 2046.1 2492.4 2905.8 3271.9 3581.1 3827.4 4006.7
Hours from 1997-07-07/13:15:00

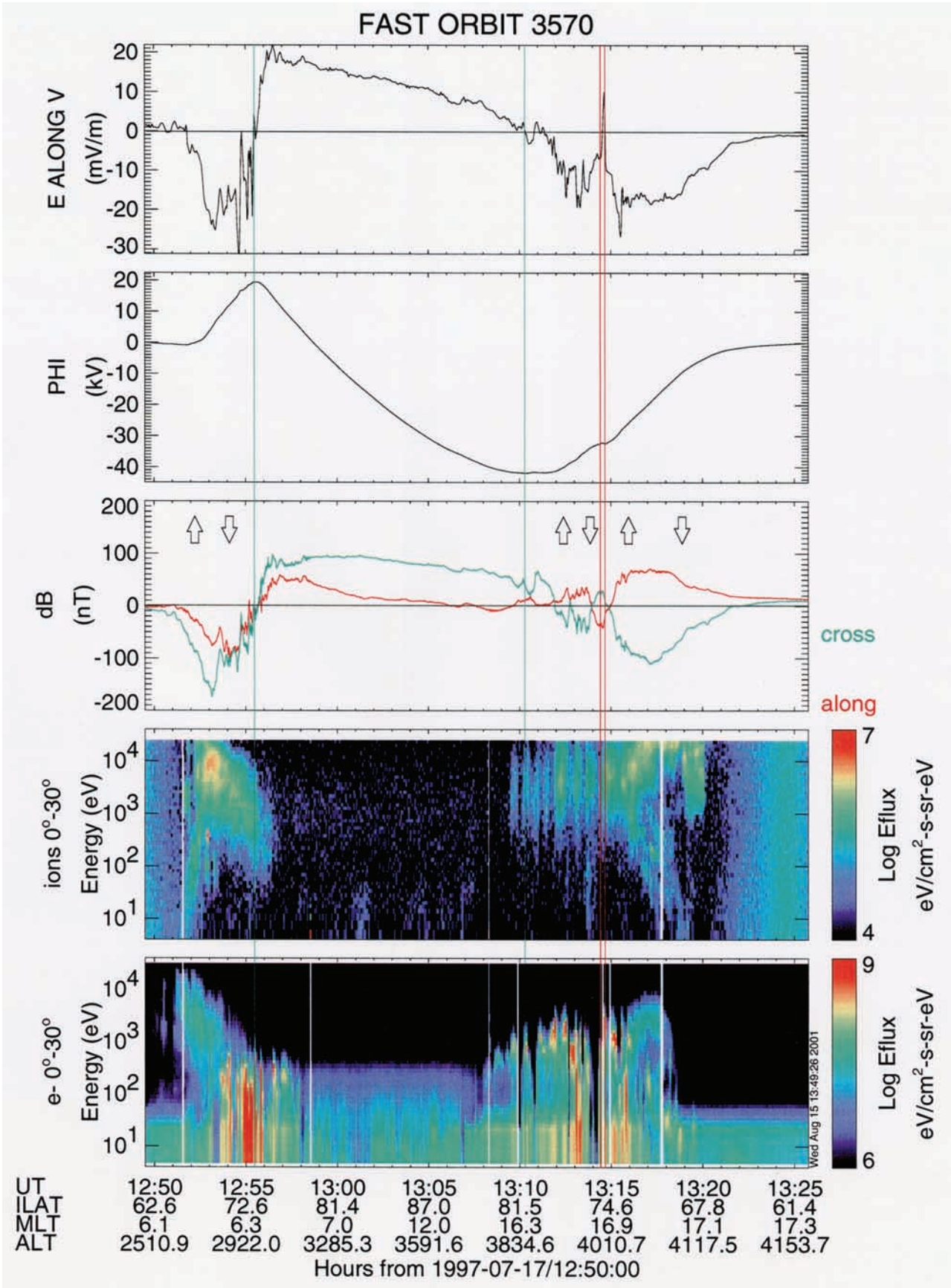

Figure 4. FAST orbit 3570. Same format as Figure 3. Four FACs are observed on the duskside for IMF B_y = 3.9 nT.

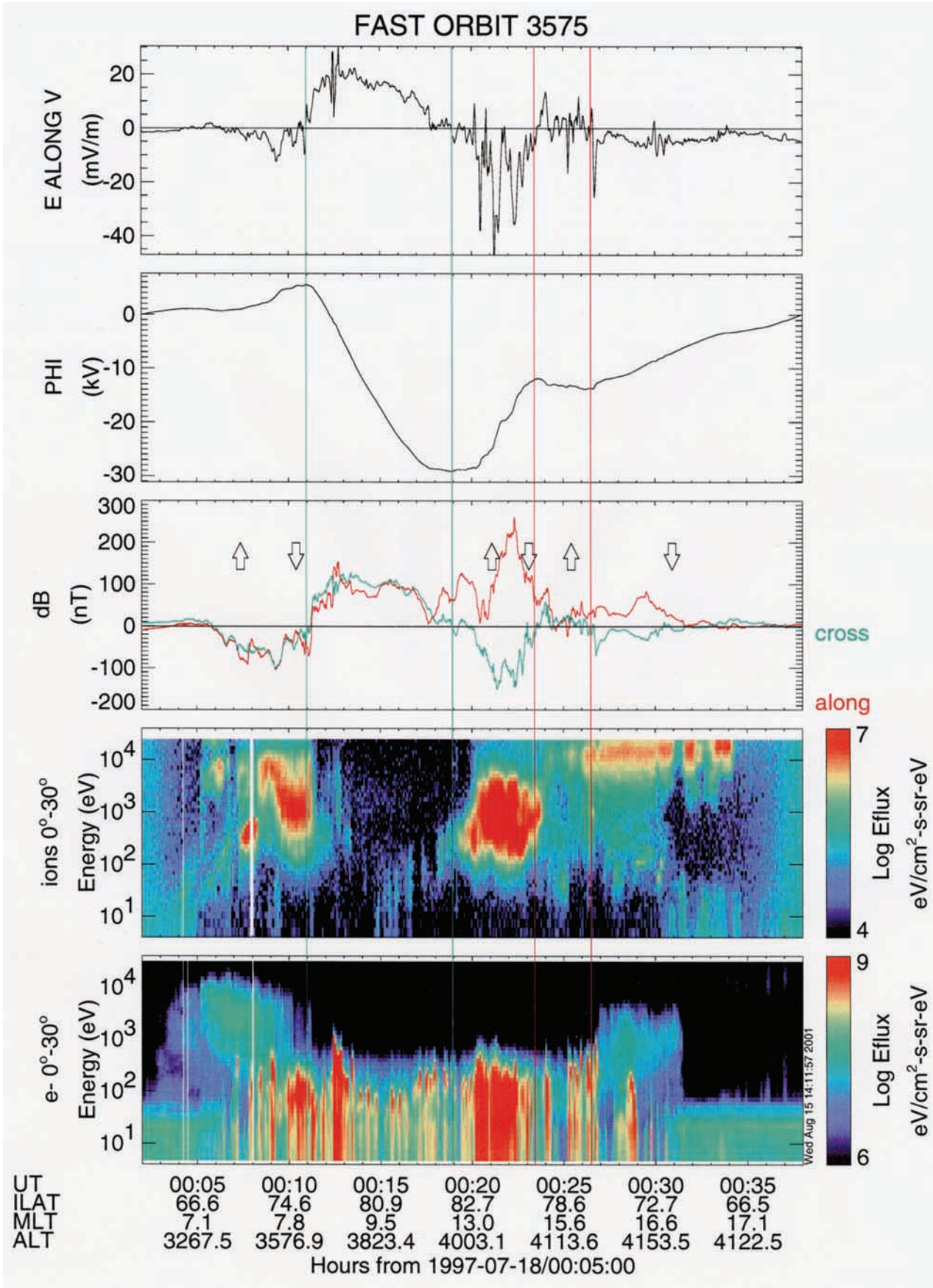

Figure 5. FAST orbit 3575. Same format as Figure 3. Four FACs are observed on the duskside for IMF B_y = 6.1 nT.